

*Drivers of sub-seasonal extreme rainfall
and their representation in ECMWF
forecasts during the Eastern African
March-to-May seasons of 2018 to 2020*

Article

Published Version

Creative Commons: Attribution-Noncommercial 4.0

Open Access

Gudoshava, M., Nyinguro, P., Talib, J., Wainwright, C., Mwanthi, A., Hirons, L. ORCID: <https://orcid.org/0000-0002-1189-7576>, de Andrade, F., Mutemi, J., Gitau, W., Thompson, E., Gacheru, J., Marsham, J., Endris, H. S., Woolnough, S. ORCID: <https://orcid.org/0000-0003-0500-8514>, Segele, Z., Atheru, Z. and Artan, G. (2024) Drivers of sub-seasonal extreme rainfall and their representation in ECMWF forecasts during the Eastern African March-to-May seasons of 2018 to 2020. *Meteorological Applications*, 31 (5). e70000. ISSN 1469-8080 doi: 10.1002/met.70000 Available at <https://centaur.reading.ac.uk/117948/>

It is advisable to refer to the publisher's version if you intend to cite from the work. See [Guidance on citing](#).

To link to this article DOI: <http://dx.doi.org/10.1002/met.70000>

Publisher: Royal Meteorological Society

All outputs in CentAUR are protected by Intellectual Property Rights law, including copyright law. Copyright and IPR is retained by the creators or other copyright holders. Terms and conditions for use of this material are defined in the [End User Agreement](#).

www.reading.ac.uk/centaur






CentAUR

Central Archive at the University of Reading

Reading's research outputs online

RESEARCH ARTICLE

Drivers of sub-seasonal extreme rainfall and their representation in ECMWF forecasts during the Eastern African March-to-May seasons of 2018–2020

Masilin Gudoshava¹  | Patricia Nyinguro² | Joshua Talib³  |
 Caroline Wainwright⁴ | Anthony Mwanthi^{1,5}  | Linda Hirons^{6,7} |
 Felipe de Andrade⁸ | Joseph Mutemi⁵  | Wilson Gitau⁵  |
 Elisabeth Thompson⁹ | Jemimah Gacheru² | John Marsham¹⁰ |
 Hussien Seid Endris¹ | Steven Woolnough^{6,7} | Zewdu Segele¹¹ |
 Zachary Atheru¹ | Guleid Artan¹

¹Climate Diagnostics and Prediction, IGAD Climate Prediction and Applications Centre, Nairobi, Kenya

²Forecasting, Kenya Meteorological Department, Nairobi, Kenya

³Hydro-Climate Risks, UK Centre for Ecology and Hydrology, Wallingford, UK

⁴School of Earth and Environmental Sciences, Cardiff University, Cardiff, UK

⁵Department of Meteorology, University of Nairobi, Nairobi, Kenya

⁶Department of Meteorology, University of Reading, Reading, UK

⁷National Centre for Atmospheric Science, University of Reading, Reading, UK

⁸Centre for Weather Forecasting and Climate Studies, National Institute for Space Research, Cachoeira Paulista, São Paulo, Brazil

⁹Applied Science, United Kingdom Met Office, Exeter, UK

¹⁰School of Earth and Environment, University of Leeds, Leeds, UK

¹¹Climate Prediction Centre, International Desk, National Oceanic and Atmospheric Administration, Washington, DC, USA

Correspondence

Masilin Gudoshava, Climate Diagnostics and Prediction, IGAD Climate Prediction and Applications Centre, Nairobi, Kenya.
 Email: masilinst@gmail.com

Funding information

Global Challenges Research Fund, African Science for Weather Information and Forecasting Techniques (SWIFT) Programme, Grant/Award Number: NE/P021077/1; Coproduction of Climate Services for East Africa (CONFER), Grant/Award Number: 869730; Intra-ACP Climate Services and Related Applications Programme, Grant/Award Number: ACP/FED/038-833; Natural Environment Research Council, Grant/Award Number: NE/X006247/1; NERC National Capability

Abstract

In recent years, Eastern Africa has been severely impacted by extreme climate events such as droughts and flooding. In a region where people's livelihoods are heavily dependent on climate conditions, extreme hydrometeorological events can exacerbate existing vulnerabilities. For example, suppressed rainfall during the March to May 2019 rainy season led to substantial food insecurity. In order to enhance preparedness against forecasted extreme events, it is critical to assess rainfall predictions and their known drivers in forecast models. In this study, we take a case study approach and evaluate drivers during March to May seasons of 2018, 2019 and 2020. We use observations, reanalysis and predictions from the European Centre for Medium-Range Weather Forecasts (ECMWF) to identify and evaluate rainfall drivers. Extreme rainfall during March to May 2018 and 2020 was associated with an active Madden–Julian

This is an open access article under the terms of the [Creative Commons Attribution-NonCommercial](https://creativecommons.org/licenses/by-nc/4.0/) License, which permits use, distribution and reproduction in any medium, provided the original work is properly cited and is not used for commercial purposes.

© 2024 The Author(s). *Meteorological Applications* published by John Wiley & Sons Ltd on behalf of Royal Meteorological Society.

International Programmes Award,
 Grant/Award Number: NC/X006263/1

Oscillation (MJO) in Phases 1–4, or/and a tropical cyclone to the east of Madagascar. On the other hand, the dry 2019 March to May MAM season, which included a delayed rainfall onset, was associated with tropical cyclones to the west of Madagascar. In general, whilst ECMWF forecasts correctly capture temporal variations in anomalous rainfall, they generally underestimate rainfall intensities. Further analysis shows that underestimated rainfall is linked to a weak forecasted MJO and errors in the location and intensity of tropical cyclones. Taking a case study approach motivates further study to determine the best application of our understanding of rainfall drivers. Communicated effectively, knowledge of rainfall drivers and forecast uncertainty will inform preparedness actions and reduce climate-driven social and economic consequences.

KEYWORDS

Eastern Africa, forecast evaluation, long rains, S2S

1 | INTRODUCTION

Over recent decades, the intensity and frequency of extreme events, such as droughts and flooding, have dramatically increased over Eastern Africa during the months of March to May (MAM), also known as the long-rains season (Chang'a et al., 2020; Kilavi et al., 2018). These extreme events have had devastating impacts on local populations. For example, they have led to localized crop damage, outbreaks of pests and diseases, food insecurity, loss of property and livestock, displacement of populations, and a large number of fatalities (NASA, 2018; Palmer et al., 2023; Reliefweb, 2020; Salih et al., 2020). From 2018 to 2020, alternating anomalous wet and dry MAM seasons were experienced over Eastern Africa (Chang'a et al., 2020). The 2018 and 2020 MAM seasons were extremely wet and led to widespread flooding, as well as exceptional river and lake levels (Kilavi et al., 2018; MacLeod et al., 2021; Marsham et al., 2020; Wanzala & Ogallo, 2020). Conversely, the MAM 2019 season was anomalously dry and caused widespread climate-induced food insecurity (Harrison et al., 2019). Whilst multiple studies have investigated the drivers of Eastern African rainfall (e.g., Finney et al., 2020; Funk et al., 2018; MacLeod et al., 2021; Talib et al., 2023), or provided a qualitative assessment of forecast skill (de Andrade et al., 2021; Endris et al., 2021), there has been minimal work assessing sub-seasonal forecasts from a case study perspective.

Unlike the October to December season, also known as the short rains, where the drivers of inter-annual rainfall variability are well known (Dutra et al., 2013; Mutai & Ward, 2000; Ogallo et al., 1988), no single large-

scale driver has been found to influence the inter-annual variability of the MAM season. Recently, Funk et al. (2018) have shown a link between the El Niño-Southern Oscillation (ENSO) and seasonal accumulations during the long rains. Strong La Nina events are followed by warmer sea surface temperatures (SSTs) in the western Pacific, referred to as the 'Western V Pattern', which strengthen the Walker Circulation and suppresses the MAM rainfall. However, the relationship is only a source of predictability for dry years. Focusing on sub-seasonal timescales, the Madden-Julian Oscillation (MJO, Berhane & Zaitchik, 2014; Hogan et al., 2015; Zaitchik, 2017; Finney et al., 2020; Maybee et al., 2023; Pohl & Camberlin, 2006; Talib et al., 2023), tropical cyclones (Finney et al., 2020) and equatorial waves (MacLeod et al., 2021) have all been found to be major drivers of sub-seasonal variability within the long rainy season. The link between the MJO and extreme rainfall has been demonstrated in a number of studies (e.g., Kilavi et al., 2018; MacLeod et al., 2021; Maybee et al., 2023; Pohl & Camberlin, 2006). When the MJO is active in Phases 2–4, precipitation is enhanced; meanwhile, when the MJO is in Phases 6–8, precipitation is suppressed. Finney et al. (2020) highlight that the position of tropical cyclones in the south-west Indian Ocean influences Eastern Africa rainfall. Their study found that tropical cyclones located to the east of Madagascar were associated with westerly winds around Lake Victoria and enhanced Eastern Africa rainfall, whereas cyclones located to the west of Madagascar drive easterly anomalous winds and reduce rainfall. The study also concluded that extreme rainfall is most favourable when the MJO is active in Phases 2 or 3 and a tropical cyclone is located in

the south-west Indian Ocean to the east of Madagascar. Alongside the MJO state providing a source of rainfall predictability, MacLeod et al. (2021) also found that extreme rainfall is favoured during days with an active equatorial Kelvin wave due to enhanced westerly wind anomalies and moisture transported from continental to Eastern Africa.

Evaluations of sub-seasonal forecasts across Eastern Africa illustrate that forecast skill is high up to a two-week lead time (de Andrade et al., 2021; Endris et al., 2021). Endris et al. (2021) evaluated the skill of 11 global climate models, including Météo-France/Centre National de Recherche Meteorologiques (CNRM); the European Centre for Medium-Range Weather Forecasts (ECMWF), National Centers for Environmental Prediction (NCEP) and the U.K. Met Office (UKMO). They found, and consistent with de Andrade et al. (2021), that ECMWF forecasts perform consistently better than other models. Several studies have also investigated whether forecasts reliably predict sub-seasonal rainfall drivers. Regarding the MJO, studies have found that predictive skill is sensitive to the MJO state at forecast initialization. When a forecast model is initialized with a strong MJO, predictive skill is higher than when initializing with a weak or inactive MJO (Kim et al., 2014; Lim et al., 2018). MacLeod et al. (2021) found that ECMWF and UKMO models accurately represent the teleconnection between the MJO and Eastern Africa rainfall. Given the low skill of seasonal forecasts at predicting MAM rainfall (MacLeod, 2018, 2019; Mwangi et al., 2014), the requirement for utilizing sub-seasonal forecasts to develop early warning systems is enhanced (Gudoshava et al., 2022; Hirons et al., 2021; White et al., 2017). For example, Kilavi et al. (2018) highlight that the seasonal forecast issued in February before MAM 2018 favoured near-normal conditions across the majority of Eastern Africa. However, seasonal rainfall accumulations were amongst the wettest on record.

Improving our understanding of the representation of the drivers in climate models at sub-seasonal timescales is key to developing early warning/early action systems and enhancing the resilience of populations within Eastern Africa. In this study, we focus on rainfall predictability during three recent long rainy seasons of 2018, 2019 and 2020. We take a case study approach to interrogate the ability of sub-seasonal forecasts at capturing these high-impact events. Through such a case study approach, we are also able to compare the interacting large-scale sub-seasonal drivers during these three high impacts, but contrasting, long rainy seasons. The study has two main components, including (1) an evaluation of ECMWF forecasts at predicting rainfall anomalies; and (2) an

investigation into the representation of known sub-seasonal rainfall drivers during each of the MAM seasons.

Section 2 outlines the datasets and methods used to characterize rainfall during each of the MAM seasons and evaluate forecast quality. Section 3 provides a detailed discussion on sub-seasonal rainfall variability during the three long rainy seasons (Section 3.1); the success of ECMWF rainfall forecasts at predicting anomalous rainfall and the forecast representation of sub-seasonal atmospheric drivers (Section 3.2). A summary and conclusions are given in Section 4.

2 | DATA AND METHODS

2.1 | Observations and reanalysis data

Several satellite-based rainfall observational datasets are available over the Eastern Africa region (Huffman et al., 2007; Ashouri et al., 2015; Funk et al., 2015; Joyce et al., 2004; Maidment et al., 2014; Novella & Thiaw, 2013; Tarnavsky et al., 2014; Thorne et al., 2001). Dinku et al. (2018) evaluated multiple satellite datasets over the region against rain gauge observations and showed that the Tropical Applications of Meteorology using SATellite and ground-based observations (TAMSAT) performed better at the daily timescale in comparison with the Climate Hazards Group Infrared Precipitation (CHIRP), CHIRP combined with station observations (CHIRPS) and African Rainfall Climatology version 2 (ARC2) datasets. Because of minimal errors at a daily timescale, we use the TAMSAT dataset to characterize sub-seasonal rainfall variability and evaluate forecast output. TAMSAT datasets are available from 1983 to the near present (Maidment et al., 2014) at a spatial resolution of 0.0375° (approximately 4 km). The ECMWF fifth-generation reanalysis (ERA5, Hersbach et al., 2020) datasets were used in evaluating the atmospheric fields. ERA5, computed using four-dimensional variational data assimilation and cycle 41r2 of the Integrated Forecasting System, provides a detailed record of the global atmosphere, land and ocean waves (Hersbach et al., 2018; Hersbach 2019). The global dataset is available from 1940 to the near present at a 0.25° horizontal resolution. In this study, we use hourly atmospheric data on seven pressure levels (200, 300, 500, 700, 850, 925 and 1000 hPa). When comparing precipitation errors, TAMSAT observations are re-gridded to a horizontal resolution of 1.5° using a first-order conservative interpolation scheme to be consistent with the resolution of ECMWF forecasts (Section 2.2). Regarding ERA5, we downloaded the

reanalysis data at the same horizontal resolution as the forecasts.

The Dipole Mode Index (DMI), an indicator of the Indian Ocean Dipole (IOD, Saji et al., 1999; Webster et al., 1999), and the Oceanic Niño Index (ONI), an indicator for the ENSO, are obtained from the National Oceanic and Atmosphere Administration Climate Prediction Centre (NOAA CPC) website. Although the IOD and ENSO are not major drivers of inter-annual variability during the long rains, recent studies have shown that the influence of large-scale oceanic drivers on the characteristics of long rains seasons is mediated by anthropogenic forcing or multi-decadal natural variability (Anderson et al., 2023; Funk et al., 2014; Park et al., 2020). SSTs are extracted from the Optimum Interpolation Sea Surface Temperature (OISST v2.1) analysis (Banzon et al., 2020; Reynolds, 1993). SST-based datasets are available from 1981 to near present at a horizontal resolution of 0.25° . Observed MJO indices are obtained from the Australian Bureau of Meteorology (Wheeler & Hendon, 2004). These MJO indices are computed using zonal winds at 850 and 200 hPa from the reanalysis product produced by the National Centers for Environmental Prediction (NCEP) and the National Center for Atmospheric Research (NCAR; Kalnay et al., 1996), and daily-mean outgoing long-wave radiation observations (Liebmann & Smith, 1996) from the NOAA. The two leading empirical orthogonal functions associated with these variables, and the corresponding principal components (PC1 and PC2), are used to diagnose the phase and amplitude of the MJO (Wheeler & Hendon, 2004). The location of the observed active tropical cyclones in the Indian Ocean during each of the studied MAM seasons is obtained from the International Best Track Archive for Climate Stewardship (IBTrACS) best-track version 4 (Knapp et al., 2018).

2.2 | Sub-seasonal forecasts

The Global Challenges Research Fund (GCRF) African Science for Weather Information and Forecasting Techniques (African SWIFT) project (Parker et al., 2022) was 1 of 16 projects that took part in the Sub-seasonal to Seasonal (S2S) prediction project (Vitart et al., 2017) Real-time Pilot Initiative. As part of the initiative, African SWIFT carried out a two-year sub-seasonal forecasting testbed: a forum where new bespoke sub-seasonal forecast products are co-produced and operationally trialed in real-time (Gudoshava et al., 2022; Hirons et al., 2021, 2023). During the testbed, the ECMWF model was utilized because past studies have shown that skill of the model is relatively high over the region in comparison with other models (de Andrade et al., 2021; Endris

et al., 2021; Vigaud et al., 2018). The ECMWF issues sub-seasonal forecasts twice a week on Monday and Thursday. We utilize the Monday initialization for the evaluation of the model consistent with the initialization that was utilized operationally in the forecasting testbed (Gudoshava et al., 2022; Hirons et al., 2021, 2023). The ECMWF forecast has a run length of 46 days and 51 ensemble members. The hindcast in ECMWF consists of 11 ensemble members for the past 20 years, and it is based on real-time forecast dates.

2.3 | Methods

Weeks with extreme rainfall in studied MAM seasons were identified using TAMSAT estimates. The weeks with the highest rainfall anomalies during each MAM season were classified as an 'extreme week'. These weeks are later shown in Figures 3 and 4. To evaluate MJO forecasts, we calculate forecasted MJO indices using a modified method described in Gottschalck et al. (2010). We project meridionally-averaged (-10° to 0° N latitude) 850 and 200 hPa zonal winds, alongside outgoing long-wave radiation anomalies, onto the empirical orthogonal function structures of Wheeler and Hendon (2004). Inter-annual MJO variability is removed by subtracting the 20-year hindcast mean of RMM indices from the previous 120 days. To compute the forecast bias, we subtract weekly-mean observed anomalies from forecast anomalies. When computing biases for each year, we use the same 20-year period for both forecasts and observations. For instance, when evaluating forecasts issued in 2020, we used 2000–2019 climatologies for both forecasts and observations. This is consistent with operational practices at ECMWF who perform reforecasts for the previous 20 years when issuing a forecast (Vitart et al., 2017).

3 | RESULTS

3.1 | Precipitation characteristics during MAM rainfall seasons in 2018, 2019 and 2020

To highlight the anomalously wet and dry MAM seasons experienced between 2018 and 2020, we first provide an overview of spatial and temporal variations in precipitation anomalies during each MAM season. Anomalies are calculated relative to a 1998–2017 climatology. This climatology includes all years used in hindcast climatologies excluding years when forecasts are evaluated (i.e., 2018, 2019 and 2020). The timespan of 20 years is consistent with operational procedures by ECMWF who

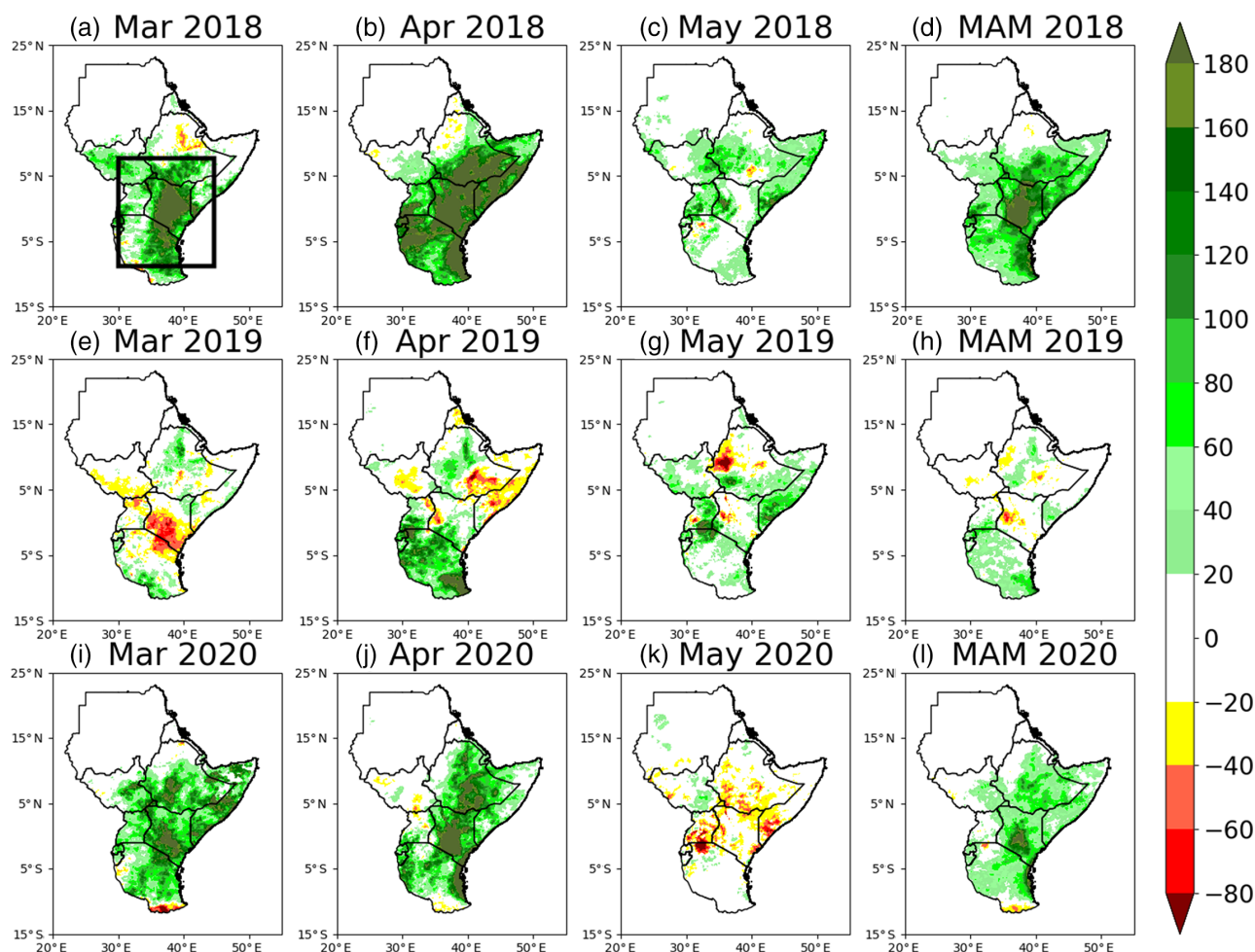


FIGURE 1 Monthly and seasonal Tropical Applications of Meteorology using SATellite and ground-based observations (TAMSAT) precipitation anomalies (mm month^{-1}) during 2018 (top), 2019 (centre), and 2020 (bottom) in March (far left), April (middle), May and March–May (far right). Anomalies are calculated using a 1998–2017 climatology. The black rectangle shown in Panel (a) denotes the area (-8 to -8° N latitude, 30 – 45° E longitude) used for computing regional means in Figures 2 and 4.

perform reforecasts for the previous 20 years relative to the forecast initialization date (Vitart et al., 2017). Figure 1 shows anomalous monthly and seasonal rainfall totals across Eastern Africa during each MAM season, whilst Figure 2 illustrates daily variations in regional mean precipitation. For our regional average, we consider all land points in the rectangle of -8 to 8° N latitude and 30 – 45° E longitude, (denoted by black rectangle in Figure 1a). This is the same region that was used in Kilavi et al. (2018). In March 2018, parts of Kenya and Tanzania received enhanced rainfall, which was in excess of 180 mm compared with the climatological (1997–2017) mean (Figure 1a). The enhanced rainfall continued into April 2018 with both equatorial and southern parts of Eastern Africa being wetter than usual (Figure 1b), and slightly reduced in May (Figure 1c). Daily rainfall in 2018 is consistently above the 90th percentile, this is especially so during the month of April (Figure 2a). Focusing on the daily accumulations, we observe a steep increase in

cumulative rainfall during April 2018, and by the end of the rainfall season, the total amount of accumulated rainfall (510 mm) is almost double the climatological mean (288 mm; Figure 2b). Subsequently, the 2018 long rainy season was one of the wettest MAM seasons on record (Kilavi et al., 2018). Moving onto MAM 2019, most of Eastern Africa received suppressed or near-normal rainfall during March 2019, with southern parts of Tanzania and the Ethiopian highlands being an exception (Figure 1e). Anomalous dry conditions continued until mid-April (Figure 2c). From mid-April to the end of the season (May), Eastern Africa received enhanced rainfall, with 21 days exceeding the climatological mean (Figure 2c). For most of MAM 2019, the total rainfall was below climatology; however, rainfall partially recovered in May (Figure 2d). Overall, deficit rainfall during the start of the season (Figures 1e,f and 2c) led to an anomalously dry MAM 2019 season, particularly over parts of central to western Kenya, southern South Sudan and

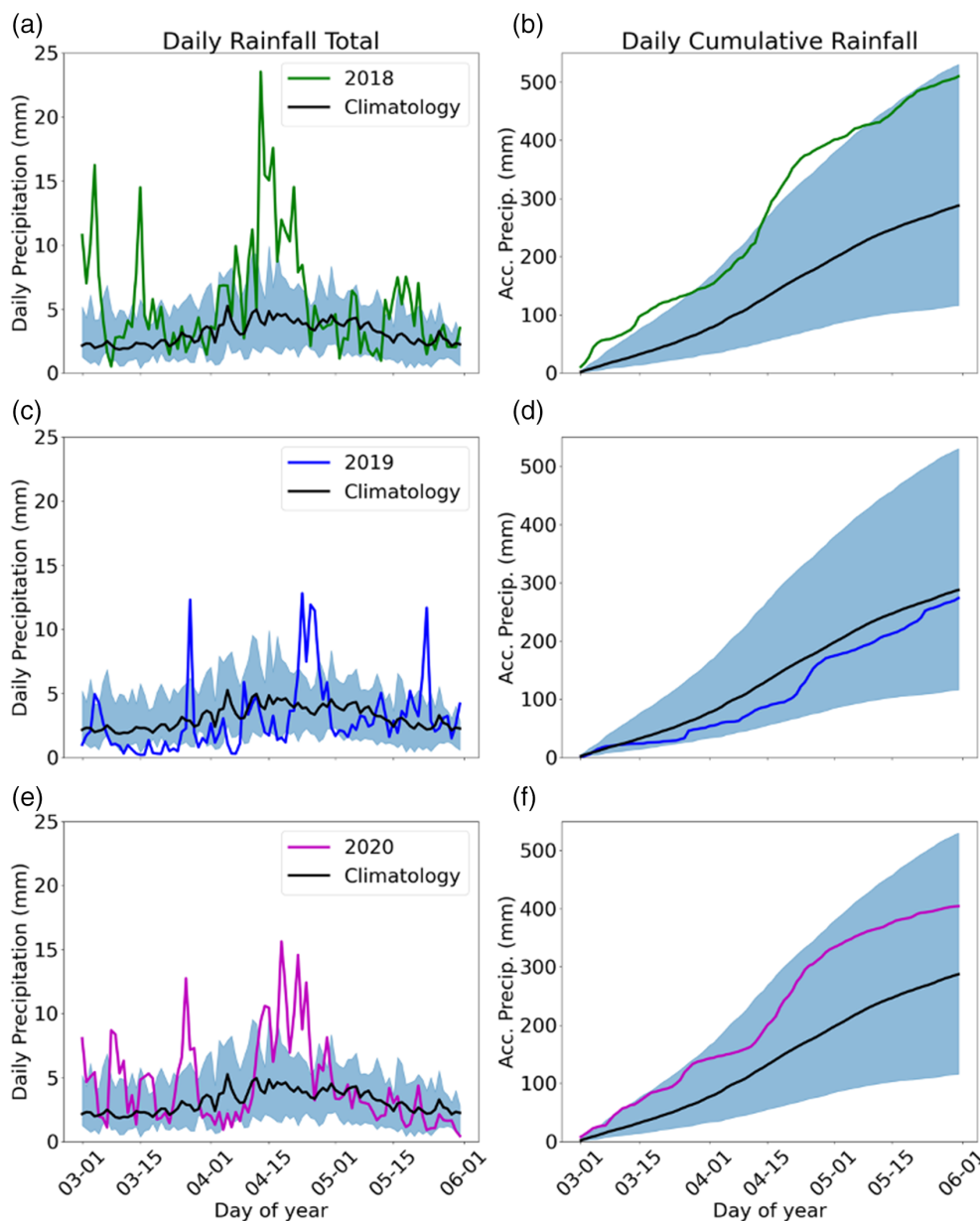


FIGURE 2 Regional mean (-8 to -8° N latitude, 30 – 45° E longitude) Tropical Applications of Meteorology using SATellite and ground-based observations (TAMSAT) precipitation during March to May (MAM) (top) 2018, (centre) 2019 and (bottom) 2020. Left panels show daily precipitation totals (coloured, mm day^{-1}) and the 1997–2017 climatological mean (black), whilst right panels show the seasonal precipitation accumulation (coloured, mm) alongside the climatology (black). Blue cyan shading represents the 10th and 90th rainfall percentiles over the region.

western and southeastern Ethiopia (Figure 1h). In 2020, enhanced rainfall was received across most of Eastern Africa during March and April (Figures 1i,j and 2e). In particular, daily-accumulated precipitation was high during mid-April (Figure 2f). May 2020, on the other hand, was anomalously dry over parts of Uganda, Somalia, Ethiopia and Kenya (Figure 1k). Overall, the MAM 2020 season received enhanced rainfall across the majority of Eastern Africa (Figures 1l and 2f).

Whilst the 2018–2020 long rainy seasons were diverse in their seasonal characteristics, they also exhibited substantial intra-seasonal variability. To understand the possible mechanisms responsible for intra-seasonal rainfall characteristics, the influence of three sub-seasonal rainfall drivers are investigated: (1) the MJO; (2) tropical

cyclones in the south-west Indian Ocean; and (3) large-scale coupled climate phenomena such as the ENSO and IOD. Figure 3 shows regional mean (-8 to -8° N latitude, 30 to 45° E longitude, black rectangle in Figure 1a) daily precipitation accumulations (blue bars), the phase of the MJO (black dots) and dates with active tropical cyclones in the south-west Indian Ocean (coloured dots) for each MAM season. We also show ENSO (Niño 3.4) and IOD (DMI) indices during January 2017 to January 2020. Beginning our analysis by focusing on the MJO, we identify that the MJO is active and in Phases 1–4 during periods of high rainfall across Eastern Africa (Figure 3a,c,e). This is consistent with previous work that has shown that Eastern Africa rainfall is favoured when the MJO is active in Phases 2–4 (e.g., Kilavi et al., 2018;

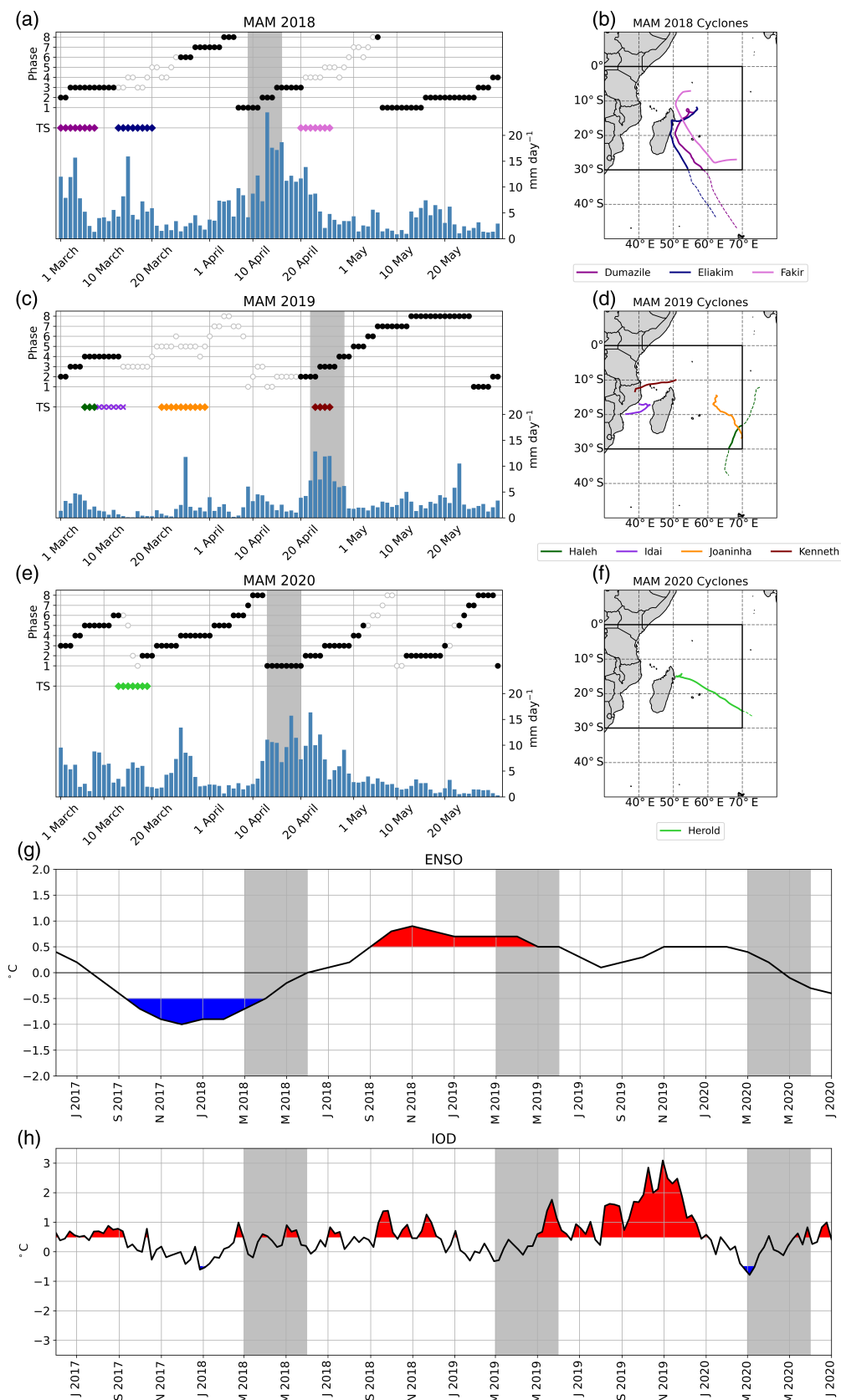


FIGURE 3 Legend on next page.

MacLeod et al., 2021; Vellinga & Milton, 2018). We particularly note that the MJO is active and in Phases 1–4 during each of the season's wettest week (denoted by grey shading, Figure 3). Focusing on MAM seasons in 2018–2020 highlights that the passage of MJO convection can modulate local rainfall.

Consistent with Finney et al. (2020), we find that the position and track of tropical cyclones in the south-west Indian Ocean mediate the impact of tropical cyclones on Eastern Africa rainfall during the 2018, 2019 and 2020 MAM seasons. Tropical cyclones in the south-west Indian Ocean impact Eastern Africa rainfall via changes in zonal wind and moisture flux convergence. Of particular importance to anomalous wet conditions across Eastern Africa are cyclones to the east of Madagascar, which lead to westerly wind anomalies and enhance moisture transport from continental to Eastern Africa. Cyclones Dumazile, Eliakim and Fakir in 2018, and cyclone Herold in 2020, were located in the east of Madagascar and associated with enhanced East African rainfall (Figure 3b,f). In 2019, on the other hand, cyclone Idai, located in the Mozambique Channel (Figure 3d), was associated with reduced rainfall over Eastern Africa and a delayed long rain onset (Figure 3c). One month after cyclone Idai made landfall, towards the end of April 2019, cyclone Kenneth formed to the north of Madagascar (Figure 3d) and led to enhanced Eastern Africa rainfall (Figure 3c). Cyclones Johaninah and Haleh, on the other hand, both of which originated further east, did not have an impact on East African rainfall. Our case study analysis of MAM rainfall seasons during 2018–2020 suggests that the impact of the MJO on Eastern African rainfall is modulated by tropical cyclones. However, the modulation of MJO-associated rainfall anomalies by tropical cyclones is sensitive to the tropical cyclone location. We observe excessive rainfall during weeks when both the MJO is active in Phases 1–4 and a tropical cyclone is present to the east or north of Madagascar (Figure 3a,c). For instance, excessive rainfall is observed between the 1st and 7th of March 2018, which coincides with an active MJO in Phases 2 and 3 and cyclone Dumazile. However, when the MJO is active and a tropical cyclone is located to the west of Madagascar, we observe suppressed rainfall (Figure 3c).

For example, during tropical cyclone Idai, 8–14 March 2019, daily rainfall was suppressed even though the MJO was active and in Phase 4.

Although previous studies demonstrate a limited influence of the ENSO and IOD on MAM rainfall (Gudoshava & Semazzi, 2019; Indeje et al., 2000), we investigate whether the state of these two climate drivers may have played a role in rainfall characteristics during the 2018–2020 MAM seasons. Whilst La Niña conditions are typically associated with below-average Eastern Africa rainfall during the MAM season (Funk et al., 2019), we find that even though the 2018 MAM season was preceded by La Niña conditions (Figure 3g), an exceptional wet MAM season occurred (Figures 1d and 2b). In May 2018, the IOD is weakly positive (Figure 3h). Throughout the MAM season in 2018, SSTs over the Indian Ocean remained cooler than usual (Figure S1a,d,g), with slightly warmer than usual temperatures over the southern part of the Indian Ocean. In MAM 2019, the south-western Indian Ocean was warmer than usual (Figure S1b,e,h). The development of positive IOD state in May 2019 (Figures 3h and S1h) may have supported the recovery of the 2019 long rainy season (Figures 1g and 2c,d). This is consistent with Endris et al. (2021), who showed that warm SSTs over the western Indian Ocean is linked to enhanced rainfall in May. Additionally, Vellinga and Milton (2018) have also shown an association between west Indian Ocean SSTs and rainfall accumulations during the long rains. For MAM 2020, whilst the IOD was neutral or weak throughout most of the season (Figure 3h), Indian Ocean SSTs across the whole basin were considerably warmer than usual (Figures S1c,f,i). As rainfall was anomalously high during MAM 2020 (Figures 1l and 2f), it identifies the need to think beyond zonal Indian Ocean SST gradients. Our case study analysis of MAM 2018–2020 seasons indicates that an early formation of the positive IOD can lead to enhanced rainfall during May. However, further research, which samples a larger number of years, is required to be more conclusive. In summary, we conclude that the amplitude and phase of the MJO, as well as Indian Ocean tropical cyclones and SSTs, mediate intra-seasonal rainfall characteristics during the long rainy seasons of 2018–2020. In the following section, we

FIGURE 3 Understanding rainfall drivers during March to May (MAM) 2018, 2019 and 2020. (a–c) Regional-mean (-8 to -8° N latitude, 30 – 45° E longitude) Tropical Applications of Meteorology using SATellite and ground-based observations (TAMSAT) precipitation (blue bars, mm day^{-1}) and current phase of Madden–Julian Oscillation (MJO) (black dots). Filled and unfilled dots highlight when the MJO is active and inactive respectively (when the MJO magnitude is greater than 1). Coloured dots indicate days when a tropical cyclone is observed across East Africa or in the south-western Indian Ocean basin. The tracks for each tropical cyclone are shown in Panels (d)–(f). Panels (g) and (h) show the magnitude of the El Niño–Southern Oscillation (ENSO) (Niño 3.4 index) and the Indian Ocean Dipole (IOD) (Dipole Mode Index) during January 2017 to January 2020. For Panels (g) and (h), MAM seasons are highlighted using grey shading.

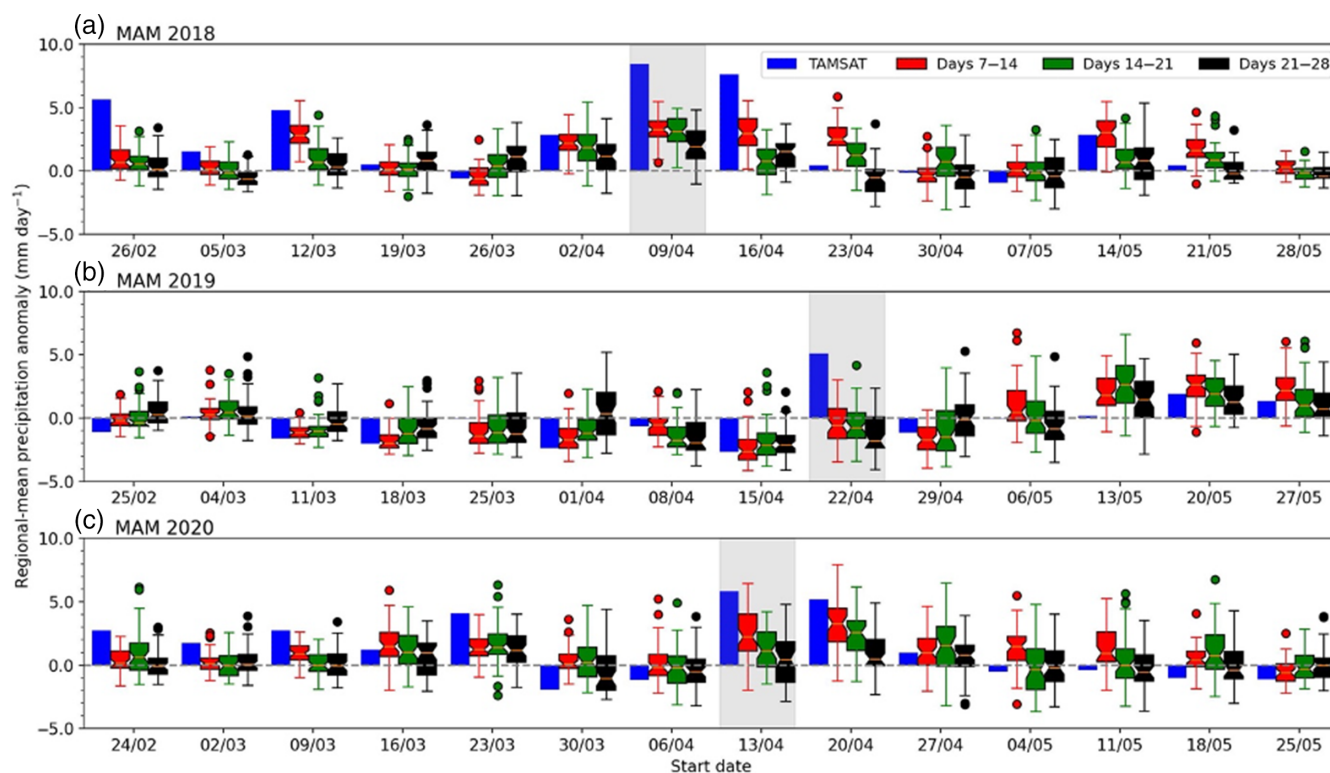


FIGURE 4 Weekly observed and forecasted regional-mean (-8 to -8° N latitude, 30 to 45° E longitude) precipitation anomalies (mm day^{-1}) during March to May (MAM) (a) 2018, (b) 2019 and (c) 2020. Blue bars denote observed Tropical Applications of Meteorology using SATellite and ground-based observations (TAMSAT) precipitation anomalies whilst box plots illustrate forecasted precipitation rates at a (red) one- (Days 7–14), (green) two- (Days 14–21) and (black) three-week (Days 21–28) lead time. Upper and lower quartiles are denoted by the top and bottom of boxes whilst box whiskers denote the 10th and 90th percentiles. Coloured dots indicate outlier ensemble members.

evaluate the representation of these intra-seasonal rainfall drivers in state-of-the-art sub-seasonal ECMWF forecasts.

3.2 | Evaluation of ECMWF sub-seasonal forecasts

3.2.1 | Evaluation of forecasted precipitation

After analysing intra-seasonal rainfall variability, and its associated drivers, during the MAM seasons of 2018–2020, here we evaluate ECMWF sub-seasonal forecasts. We partition our forecast evaluation into two components: (1) an evaluation of forecasted rainfall characteristics; and (2) an assessment of the representation of key intra-seasonal rainfall drivers. For the majority of our analysis, we evaluate forecast performance at three lead times: Week 1 (Days 7–13); Week 2 (Days 14–20); and Week 3 (Days 21–27). Figure 4 shows observed (TAMSAT) and forecasted precipitation anomalies for each week in MAM 2018, 2019 and 2020. Ensemble forecast spread is denoted using box plots.

Focusing on weeks with relatively high rainfall anomalies, Figure 4a shows that ECMWF forecasts correctly capture enhanced rainfall during the week commencing 9 April 2018. During this week, the MJO was active in Phases 1–3 (Figure 3a). Conversely, ECMWF forecasts failed to predict enhanced rainfall between the 22 and 29 April 2019 (Figure 4b). Forecasts at all lead times indicated drier than usual conditions. During this week, the MJO was active in Phases 1–3, and cyclone Kenneth was positioned to the north of Madagascar (Figure 3c,d). However, this MJO event was preceded by a period of weak MJO activity (Figure 3c), thereby a primary MJO event (Matthews, 2008), whereas active MJO conditions preceded the anomalously wet weeks in 2018 and 2020. The influence of preceding MJO conditions is explored further in Section 3.2.2. In 2020, ECMWF forecasts correctly predicted enhanced rainfall during anomalously wet weeks (i.e., weeks beginning 13 and 20 April, Figure 4c). During these weeks, the MJO was active in Phases 1–3. Whilst ECMWF forecasts correctly captured enhanced rainfall during anomalous wet weeks of 2018 and 2020, forecasted anomalous rainfall was less than observed anomalies. In general, ensemble-mean rainfall

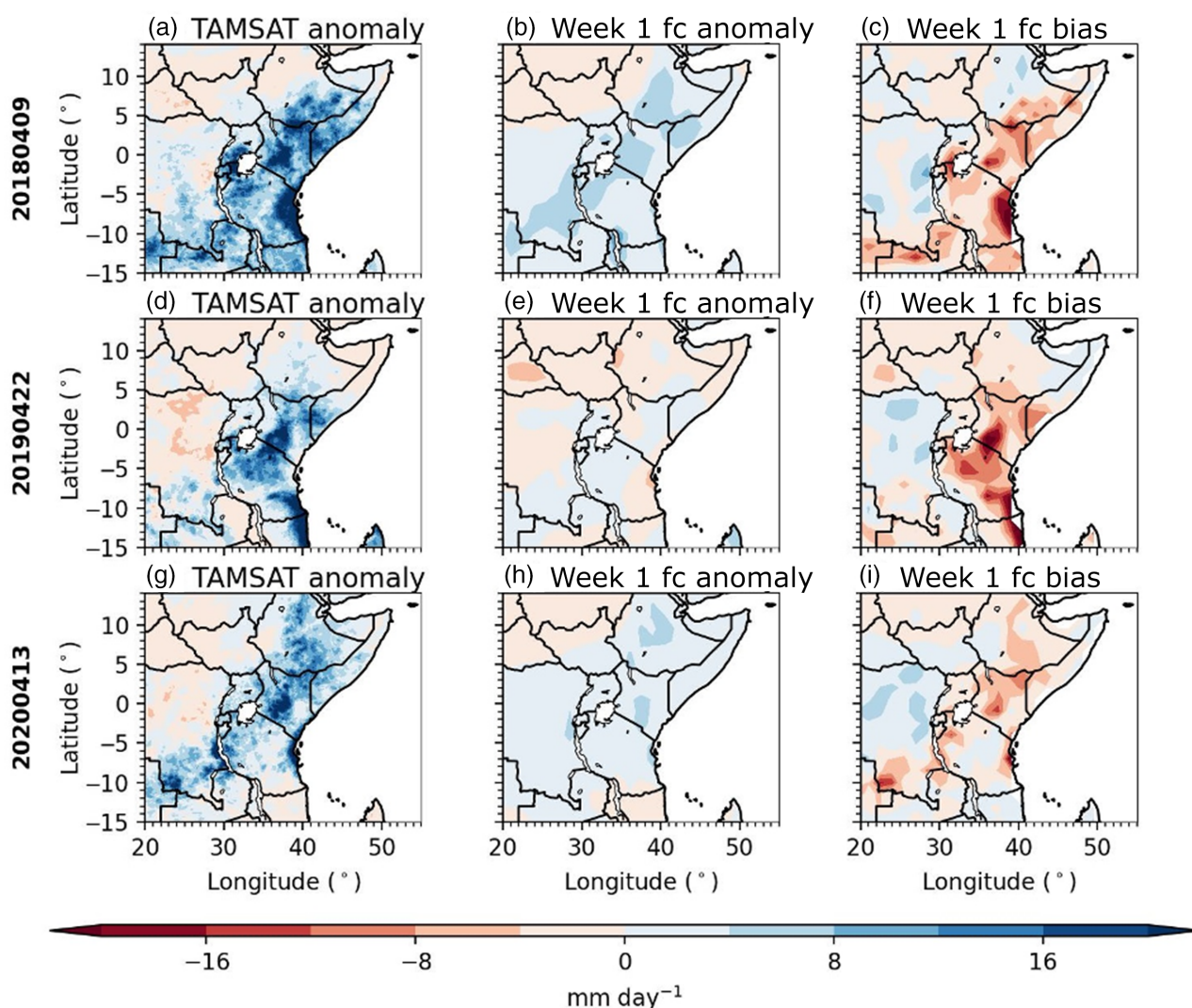


FIGURE 5 Weekly-mean observed and forecasted precipitation anomalies (mm day^{-1}) during the week beginning (a–c) 9 April 2018, (d–f) 22 April 2019 and (g–i) 13 April 2020. Panels in the first column (a, d and g) show Tropical Applications of Meteorology using SATellite and ground-based observations (TAMSAT) precipitation anomalies, whilst panels in the second (b, e, and h) and third (c, f and i) columns show forecast anomalies and biases at a 7- to 14-day lead time. To compute biases, TAMSAT data are mapped onto the same resolution as the forecasts using a first-order conservative interpolation scheme. ‘fc’ is shorthand for ‘forecast’.

anomalies were approximately a third of the observed anomaly at a one-week forecast lead time. We also note that there are weeks when Eastern Africa receives relatively normal rainfall but the forecast model overestimates rainfall anomalies (e.g., week beginning 23 April 2018 or 13 May 2019, Figure 4). Despite the model’s ability at capturing the sign of rainfall anomalies during most weeks, ECMWF forecasts do not predict the correct rainfall intensities and generally underestimate total rainfall during extreme wet events. ECMWF forecasts also tend to overestimate relatively moderate events.

Focusing on the extreme anomalous wet weeks, weeks beginning 9 April 2018, 22 April 2019 and 13 April 2020 (highlighted grey in Figure 4), we evaluated spatial variations in forecast performance. We do this by

showing the TAMSAT anomaly alongside the ensemble-mean forecast anomaly and bias at a one-week lead time in Figure 5. In the week beginning the 9 April 2018, ECMWF forecasts correctly capture anomalously wet conditions over most parts of Eastern Africa. However, predicted anomalies are not as high as those observed (Figure 5a–c), consistent with Figure 4a. Comparing the ensemble-mean forecast with TAMSAT observations shows that the ensemble mean underestimated total rainfall by up to 16 mm over parts of Tanzania (Figure 5c). In the week beginning 22 April 2019, ECMWF forecasts reproduced wet anomalies across parts of Tanzania and eastern Kenya, although with decreased magnitude compared with observations (Figure 5d,e). Additionally, dry anomalies were predicted over parts of western Kenya

and eastern Tanzania, opposite to the wet anomalies that were observed. Comparing with the extremely wet week of 2018, biases are higher over most parts of the region (Figure 5f). The sign of forecast anomalies in the week beginning 13 April 2020 are consistent with observations (Figure 5g,h). However, similar to other chosen weeks, the forecasted ensemble mean underestimates total rainfall (Figure 5i). Biases for the week commencing 13 April 2020 are lower compared with the wettest weeks of MAM 2018 and 2019 by approximately 10 mm day^{-1} . Comparing the location of forecasted rainfall errors with forecasted climatologies shows that the magnitude of errors is not due to errors in climatology (Figure S2a–d). We also compared forecast anomalies at a two- and three-week lead time (Figure S3b,c,e,fh,i). Whilst the spatial structure of forecast errors is similar with increasing lead time, the amplitude of errors increases (Figure S3).

Consistent with Figure 4, we found biases are comparable at a one- and two-week lead time (Figure S3a,b,d,e,g,h).

3.2.2 | Valuation of the large-scale drivers

It was previously noted that the forecast beginning 22 April 2019 was initialized when the MJO was inactive, whilst for the week commencing 9 April 2018, the MJO was active. As forecast skill is sensitive to the amplitude and phase of the MJO at initialization (Vitart & Molteni, 2010), we evaluated predictions of MJO characteristics during April 2018, 2019 and 2020. Figure 6 shows the ensemble spread in forecasted MJO conditions at a one-week lead time as well as the ensemble-mean MJO evolution at different week lead times. In April 2018,

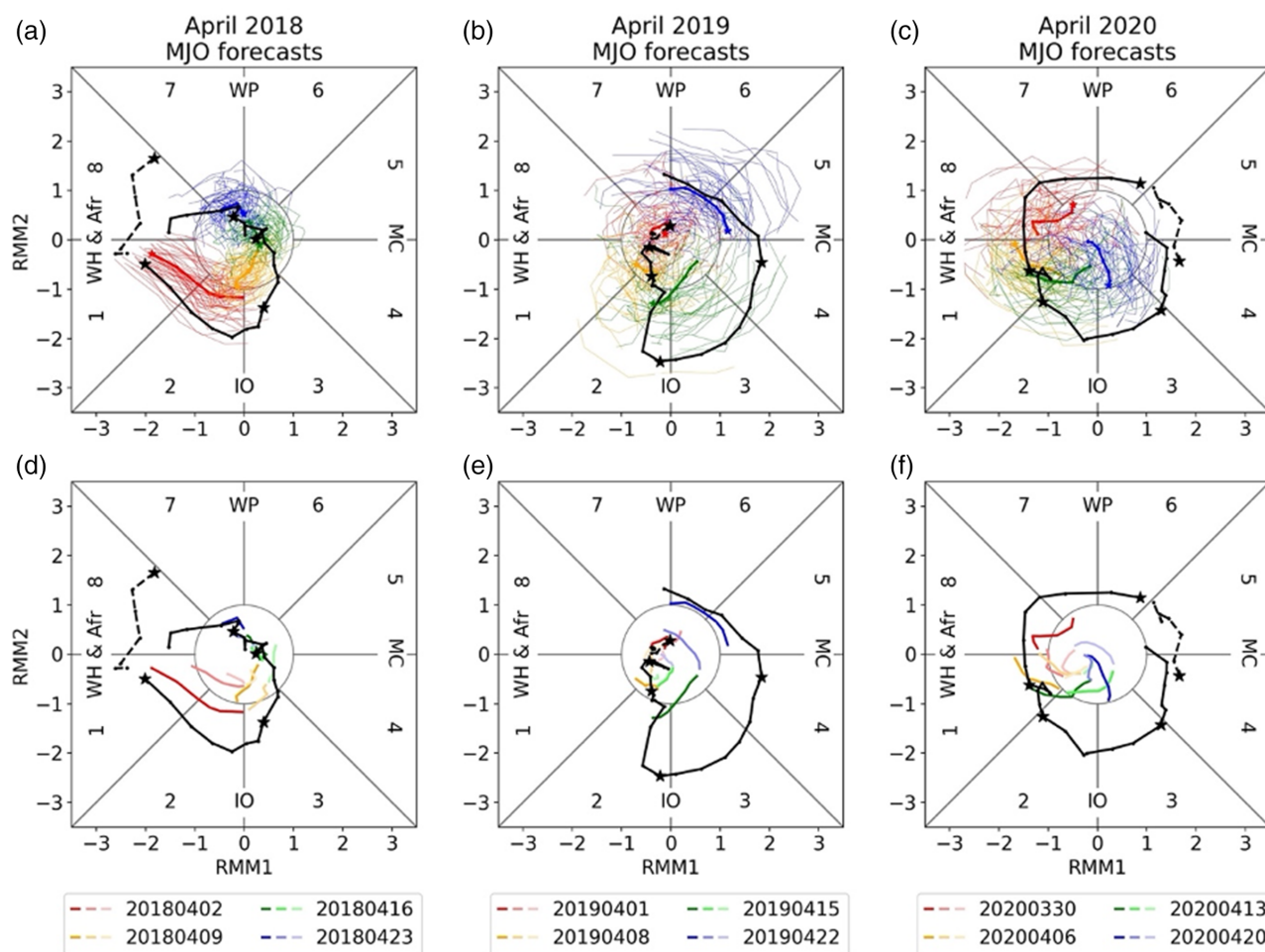


FIGURE 6 Observed Madden–Julian Oscillation (MJO) phase and intensity (black lines) alongside forecasted MJO state (coloured lines). Panels (a) to (c) show the forecasted ensemble mean (solid thick line) and individual ensemble members (solid thin lines) at a one-week lead time. Panels (d) to (f) meanwhile show the ensemble mean at different forecast lead times. A lighter shade is used to indicate increased forecast lead time. For example, in Panel (d), dark red, red and light red are used to denote the forecasted MJO state for the week commencing 2 April 2018 at a lead time of one, two and three weeks, respectively. The dashed black line in all panels denotes the observed MJO state in the week preceding the beginning of April.

ECMWF forecasts successfully predicted the phase of the MJO (Figure 6a,d). However, the ensemble mean underestimates the MJO amplitude, consistent with Kilavi et al. (2018). The underestimated MJO intensity may be partly responsible for negative rainfall errors. Whilst forecasts correctly capture weeks when the MJO is inactive in April 2019, most ensemble members incorrectly predict an inactive MJO when it was active in Phases 2–4 during the week commencing 15 April 2019 (Figure 6b,e). MJO biases during this particular week may have possibly contributed to underestimated forecasted rainfall. ECMWF forecasts also perform poorly at predicting an active MJO during the month of April 2020 (Figure 6c,f). This may be due to low predictability of the

MJO state when it initiates in the Maritime Continent (Kim et al., 2014).

The vertically integrated moisture flux divergence (VIMFD) is an important indicator of regions that are likely to receive rainfall. To further explore the ability of ECMWF forecasts at predicting heavy rainfall weeks in April 2018, 2019 and 2020, we investigate temporal and spatial patterns of forecasted VIMFD. In Figure 7, we compare the ensemble mean of forecasted VIMFD with that calculated from ERA5. For both ERA5 and forecasts, we calculate VIMFD using atmospheric data on 200, 300, 500, 700, 850, 925 and 1000 hPa pressure levels. In general, anomalies in VIMFD are underestimated by the ensemble mean of ECMWF forecasts (Figure 7). For

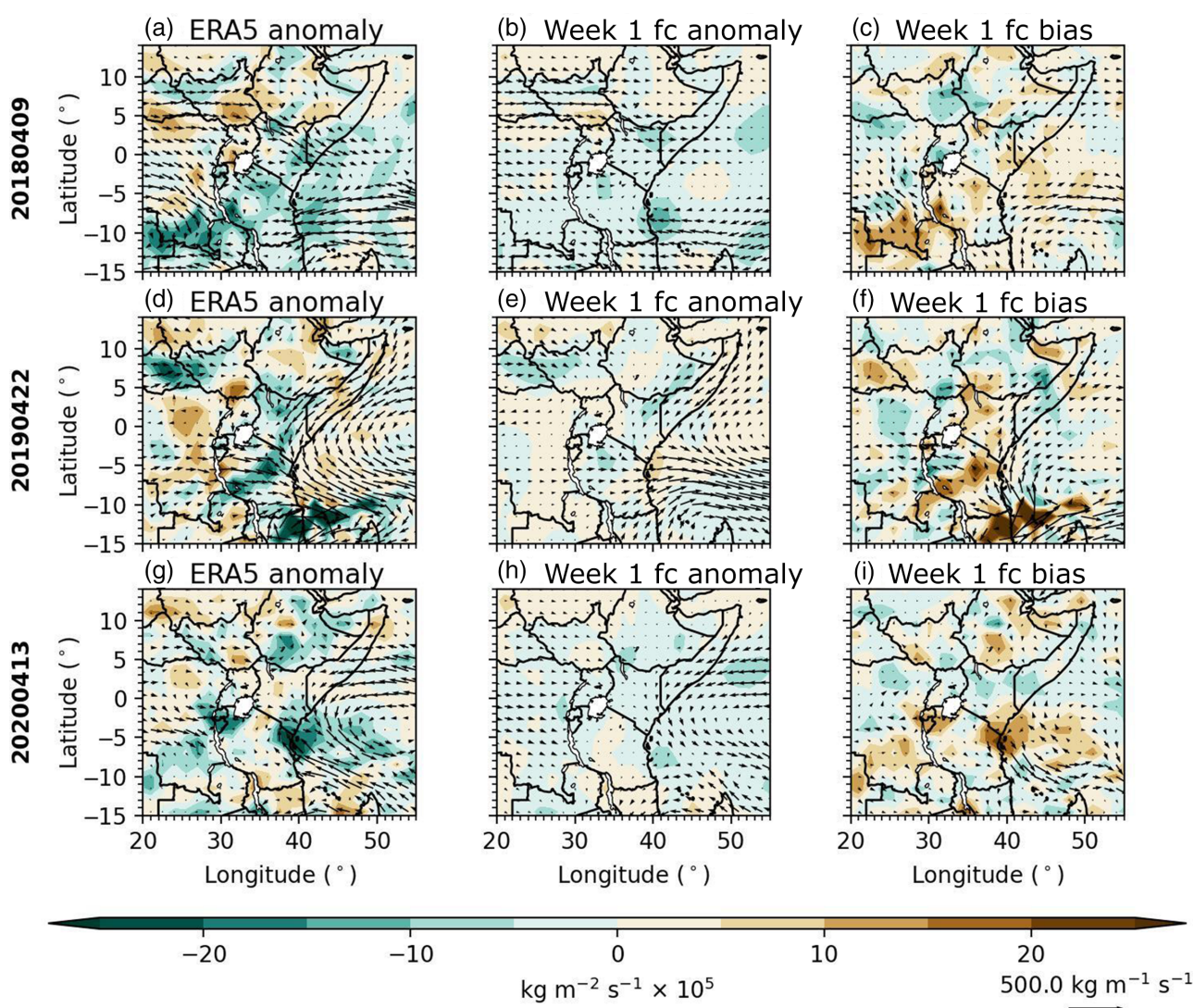


FIGURE 7 Weekly-mean ERA5 and forecasted VIMFD anomalies (filled, $\text{kg m}^{-2} \text{s}^{-1}$) and vertically integrated moisture fluxes (arrows, $\text{kg m}^{-1} \text{s}^{-1}$) during the week beginning (a–c) 9 April 2018, (d–f) 22 April 2019 and (g–i) 13 April 2020. Panels in the first column (a, d and g) show ERA5 anomalies, whilst panels in second (b, e and h) and third (c, f and i) columns show forecasted anomalies and biases at a one-week lead time. ‘fc’ is shorthand for ‘forecast’.

example, in the week beginning 9 April 2018, ERA5 shows moisture convergence across coastal regions of the equatorial sector (5° S to 5° N, Figure 7a); meanwhile, whilst one-week lead-time forecasts capture the correct anomalous spatial patterns, magnitudes in anomalous VIMFD are smaller compared with ERA5 (Figure 7b,c). The inability for ECMWF forecasts to capture the magnitude of anomalous moisture flux convergence is a consistent error in the forecast model as forecasted climatologies in the moisture flux convergence is much smaller compared with observations (Figure S2e–h). Forecast skill also decreases with increasing lead time (Figure S4a–c), with the three-week forecast indicating the highest biases (Figure S4c). Similar errors in the magnitude of VIMFD anomalies are also observed during weeks commencing 22 April 2019 and 13 April 2020 (Figure 7d–7i). Consistent with 2018, the biases in VIMFD in 2019 and 2020 also increase with increase in lead times (Figure S4d–i). Relatively weak forecasted VIMFD anomalies could partly explain the inability of ECMWF forecasts at capturing the magnitude of rainfall anomalies during extreme weeks (Figure 4).

In Section 3.1, we identified that tropical cyclones in the south-west Indian Ocean partly mediate intra-seasonal rainfall characteristics during the long rains of 2018–2020. For instance, cyclone Eliakim was associated with anomalous heavy rainfall during March 2018 (Figure 3a). To evaluate the representation of tropical cyclones influencing Eastern Africa rainfall, we selected three weeks with which a tropical cyclone was present in the south-west Indian Ocean, in the vicinity of Madagascar. Our chosen weeks commence on 12 March 2018, 22 April 2019 and 9 March 2020 when Eliakim, Kenneth and Herold were active, respectively. Figure 8 shows mean sea level pressure and 700 hPa wind anomalies in ERA5 and the ensemble mean of ECMWF forecasts at a one-week lead time. Focusing on tropical cyclone Eliakim, whilst forecasts did not capture the cyclone strength, they did predict the location and presence of a tropical cyclone as well as anomalous westerlies across the Congo (Figure 8a–c, and further supported by forecasted storm tracks in Figure S5a). This conclusion is consistent with Figure 4a, which shows that at a one-week lead time anomalous wet conditions are predicted but underestimated. Conversely, ECMWF forecasts fail to capture cyclone Kenneth, the associated anomalous westerlies across the Congo (Figures 8d–f and S5b) and wetter-than-normal conditions (Figures 4b and 5d–f). Figure S5b shows that many of the ensemble members did not contain a detectable tropical storm/hurricane track that week. For the week commencing 9 March

2020, ECMWF forecasts have a weak representation of tropical cyclone Herold (Figures 8g–i and S5c). Given that forecasts typically underestimate wet conditions when a tropical cyclone is present in the south-west Indian Ocean (Figure 4c), we hypothesize that this error is associated with a weak or minimal prediction of a tropical cyclone. Therefore, the forecast model's ability at predicting the presence and strength of tropical cyclones in the south-west Indian Ocean affects predictions of Eastern Africa rainfall. We also note that the inability for the forecast model to correctly predict a tropical storm is not associated with consistent biases in mean sea level pressure as observed and forecasted climatologies are similar (Figure S2i–l).

4 | DISCUSSION AND CONCLUSIONS

In light of an increasing awareness and demand for accurate and actionable S2S forecasts across sub-Saharan Africa (Hirons et al., 2021), in this study, we assess the ability of European Centre for Medium-Range Weather Forecasts (ECMWF) S2S forecasts at representing extreme rainfall and its key drivers during three long rainy seasons (2018–2020) in Eastern Africa. Better understanding the link between large-scale drivers and local high-impact weather has the potential to improve S2S forecasts and enhance early warning/early action systems. The 2018 and 2020 March to May (MAM) seasons were wetter than average, with MAM 2018 being one of the wettest long rainy seasons on record (Kilavi et al., 2018). Conversely, the 2019 long rainy season experienced below-average precipitation. By comparing observed rainfall anomalies with large-scale atmospheric conditions, and consistent with previous work (Finney et al., 2020; Kilavi et al., 2018; Macleod et al., 2021; Vellinga & Milton, 2018), we conclude that enhanced rainfall during the studied MAM seasons is associated with an active Madden–Julian Oscillation (MJO) in Phases 1–4, a tropical cyclone situated to the east or north of Madagascar, or a combination of both. We also find that the recovery of rainfall during the dry 2019 MAM season was associated with the development of positive Indian Ocean Dipole (IOD) conditions. Whilst continued research is warranted, and in agreement with Finney et al. (2020), we propose that the influence of the MJO on extreme Eastern Africa rainfall is modulated by tropical cyclones in the south-west Indian Ocean. We also find that suppressed rainfall and a delayed onset to the 2019 MAM season were associated with cyclone Idai to the west of Madagascar. For all three long rainy seasons studied, we find no association between El Niño

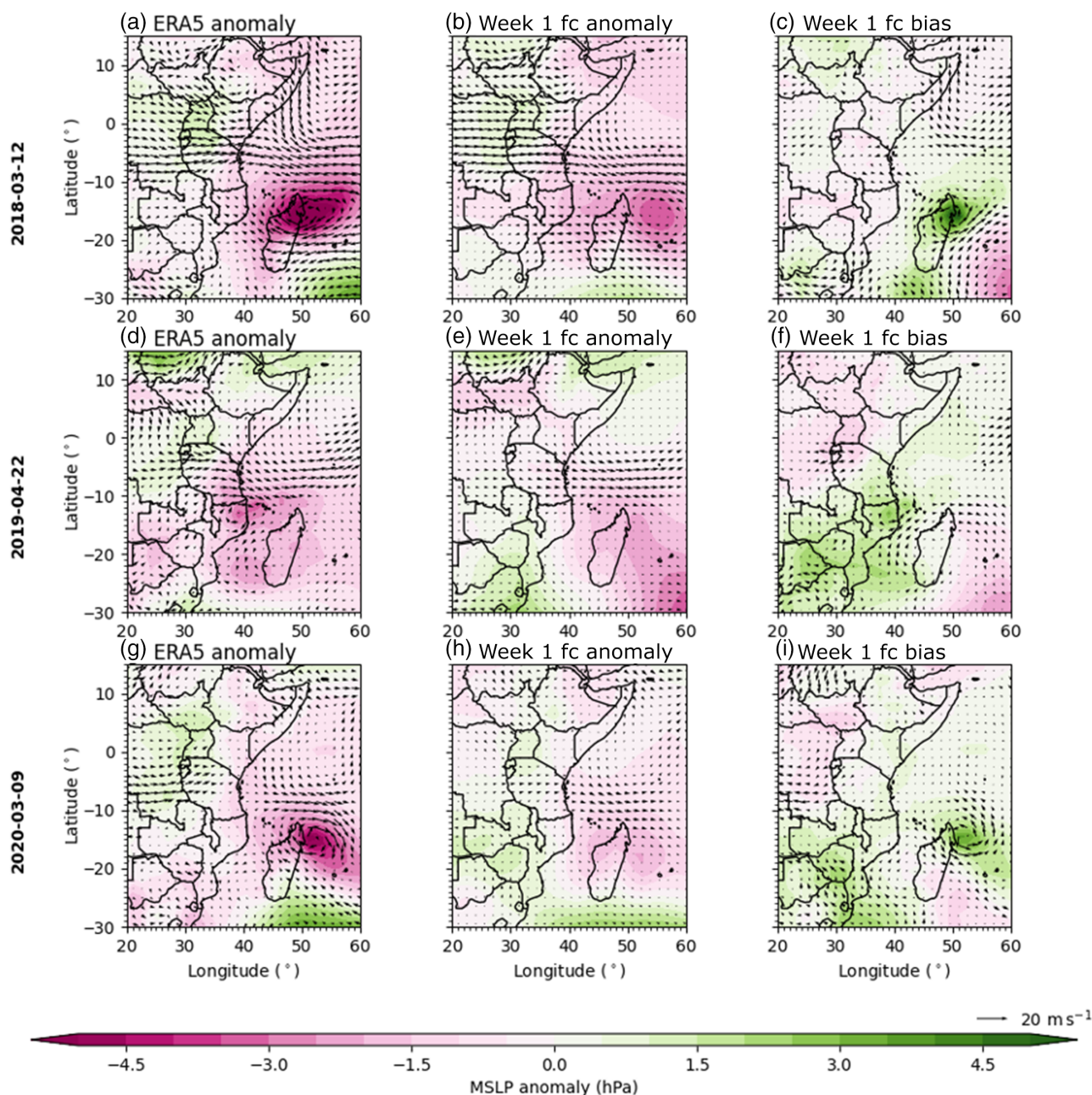


FIGURE 8 Weekly-mean ERA5 and forecasted mean sea level pressure anomalies (filled, hPa) and 700 hPa wind anomalies (arrows, m s^{-1}) during the week beginning (a–c) 3 March 2018, (d–f) 22 April 2019 and (g–i) 9 March 2020. Panels in the first column (a, d and g) show ERA5 anomalies, whilst panels in second (b, e and h) and third (c, f and i) columns show forecasted anomalies and biases at a one-week lead time. ‘fc’ is shorthand for ‘forecast’.

conditions and rainfall anomalies, which is consistent with previous work (Gudoshava & Semazzi, 2019; Indeje et al., 2000).

Evaluating ECMWF S2S forecasts and their ability to reproduce rainfall anomalies across Eastern Africa highlights that whilst forecasts correctly capture temporal rainfall variations, with particular success during the wettest weeks in MAM 2018 and 2020, forecasts failed to capture the magnitude of rainfall anomalies. In general,

forecasts underestimate rainfall anomalies during extreme wet weeks and overestimate precipitation during moderate events. Given that both positive and negative precipitation errors are found for different weeks, quantile or distribution mapping (Wood et al., 2004) are better suited bias correction techniques compared with linear scaling (Maraun, 2016). Spatial maps of errors during extreme wet weeks illustrate that errors are relatively large across coastal regions of Kenya

and Tanzania, and on the eastern side of the Eastern Africa highlands. This is unsurprising given that observed rainfall is more intense in these regions. Unsurprisingly, forecast errors increase with lead time (de Andrade et al., 2021; Endris et al., 2021). Focusing on weeks with extreme rainfall accumulations, ECMWF forecasts had similar skill at a one- and two-week lead time, with errors substantially increasing at a three-week lead time. A consideration of decreased skill at a three-week lead-time is required when developing actionable, user-focused early warning systems.

Alongside assessing forecasted precipitation, we also evaluated the representation of large-scale atmospheric drivers. Evaluating forecasted MJO characteristics during each week of April 2018, 2019 and 2020 reveals that whilst the MJO intensity is often weaker compared with observations, forecasts do reasonably well at capturing the MJO phase at a one-week lead time. Analysis of the forecasted ensemble mean highlights a rapid deterioration in forecasts of an active MJO. This agrees with work showing that S2S forecasts and climate models perform inadequately at representing persisting MJO events (Kim et al., 2019; Li et al., 2022; Seo et al., 2009). Our case study analysis is also consistent with other studies showing that an active MJO is more likely to be forecasted when the model is initialized with an active MJO (Kim et al., 2019; Vitart & Molteni, 2010). For instance, the model performs best during April 2018 compared with April 2019 and 2020, as the beginning of April 2018 was characterized by an active MJO.

In light of Finney et al., 2020, we also evaluated the forecasted influence of Indian Ocean tropical cyclones on extreme rainfall. In general, forecasts with a better tropical cyclone representation, and associated wind anomalies across continental Africa, did a better job at capturing rainfall anomalies. However, the forecasted tropical cyclone intensity is often too weak, with the location of forecasted tropical cyclones substantially varying. Our case study analysis is in agreement with Kolstad 2021, who found that only 5% of ECMWF ensemble members predicted local wind speed maxima and sea level pressure minima in the Mozambique Channel. Lee et al. (2020) also showed that skill in forecasting tropical cyclones is poor after two weeks. Given that rainfall is sensitive to the moisture flux convergence, we also evaluated spatial variations in the vertically integrated moisture flux convergence. In general, ECMWF S2S forecasts correctly predict spatial variations in the anomalous moisture flux convergence. However, anomalies are underestimated when considering the ensemble mean. Unsurprisingly, given concluded rainfall errors, biases in the moisture flux convergence increase with forecast lead time. To further develop S2S forecasts across Eastern Africa, a greater understanding of the observed and forecasted relationship

between moisture flux convergence and rainfall is required (Kolstad, 2021; Lee et al., 2020).

Future work can further explore the links between local high-impact weather and large-scale sub-seasonal atmospheric drivers. A better understanding of these links, and the associated regime-dependent skill, is crucial for informing the co-development of reliable and actionable early warnings for the region.

AUTHOR CONTRIBUTIONS

Masilin Gudoshava: Conceptualization (equal); formal analysis (equal); investigation (equal); methodology (equal); visualization (equal); writing – original draft (lead). **Patricia Nyinguro:** Conceptualization (equal); investigation (equal); methodology (equal). **Joshua Talib:** Conceptualization (equal); formal analysis (equal); investigation (equal); methodology (equal); visualization (equal). **Caroline Wainwright:** Conceptualization (equal); formal analysis (equal); investigation (equal); methodology (equal); visualization (equal). **Anthony Mwanthi:** Conceptualization (equal); methodology (equal); visualization (supporting). **Linda Hirons:** Conceptualization (equal); formal analysis (equal); methodology (equal). **Felipe de Andrade:** Formal analysis (equal); investigation (equal). **Joseph Mutemi:** Conceptualization (equal); methodology (equal). **Wilson Gitau:** Conceptualization (equal); methodology (equal). **Elisabeth Thompson:** Data curation (equal); resources (equal). **Jemimah Gacheru:** Conceptualization (equal); resources (equal). **John Marsham:** Methodology (equal). **Hussen Seid Endris:** Conceptualization (equal). **Steven Woolnough:** Conceptualization (equal); funding acquisition (equal); supervision (equal). **Zewdu Segele:** Conceptualization (equal); funding acquisition (equal); supervision (equal). **Zachary Atheru:** Funding acquisition (equal); supervision (equal). **Guleid Artan:** Funding acquisition (equal); supervision (equal).

FUNDING INFORMATION

This work was supported by UK Research and Innovation as part of the Global Challenges Research Fund, African Science for Weather Information and Forecasting Techniques (SWIFT) Programme, grant number NE/P021077/1. MG was also funded by the Coproduction of Climate Services for East Africa (CONFER), grant number 869730. HSE and ZA were funded by the Intra-ACP Climate Services and Related Applications Programme (CLIMSA, ACP/FED/038-833). JT was also supported by the Natural Environment Research Council as part of the NC-international programme (NE/X006247/1) delivering National Capability. LH and SW were also supported by NERC National Capability International Programmes Award NC/X006263/1.

DATA AVAILABILITY STATEMENT

The real-time data used in this study have been provided through the Subseasonal-to-Seasonal (S2S) Prediction Project Real-time Pilot. The S2S Prediction Project is a joint initiative of the World Weather Research Programme (WWRP) and the World Climate Research Programme (WCRP). ERA5 data were accessed on <https://cds.climate.copernicus.eu/cdsapp/home>. The observed cyclone tracks were obtained from International Best Track Archive for Climate Stewardship (IBTrACS) Project, Version 4 (NOAA National Centers for Environmental Information: <https://doi.org/10.25921/82ty-9e16>).

ORCID

Masilin Gudoshava  <https://orcid.org/0000-0003-0315-9271>

Joshua Talib  <https://orcid.org/0000-0002-4183-1973>

Anthony Mwanthi  <https://orcid.org/0000-0002-0365-374X>

Joseph Mutemi  <https://orcid.org/0000-0002-1763-9025>

Wilson Gitau  <https://orcid.org/0000-0002-4508-9411>

REFERENCES

- Anderson, W., Cook, B.I., Slinski, K., Schwarzwald, K., McNally, A. & Funk, C. (2023) Multiyear La Niña events and multiseason drought in the Horn of Africa. *Journal of Hydrometeorology*, 24(1), 119–131.
- Ashouri, H., Hsu, K.L., Sorooshian, S., Braithwaite, D.K., Knapp, K.R., Cecil, L.D. et al. (2015) PERSIANN-CDR: daily precipitation climate data record from multisatellite observations for hydrological and climate studies. *Bulletin of the American Meteorological Society*, 96(1), 69–83.
- Banzon, V., Smith, T.M., Steele, M., Huang, B. & Zhang, H.M. (2020) Improved estimation of proxy sea surface temperature in the Arctic. *Journal of Atmospheric and Oceanic Technology*, 37(2), 341–349.
- Berhane, F. & Zaitchik, B. (2014) Modulation of daily precipitation over East Africa by the Madden-Julian oscillation. *Journal of Climate*, 27(15), 6016–6034.
- Chang'a, L.B., Kijazi, A.L., Mafuru, K.B., Nying'uro, P.A., Ssemujju, M., Deus, B. et al. (2020) Understanding the evolution and socio-economic impacts of the extreme rainfall events in March-May 2017 to 2020 in East Africa. *Atmospheric and Climate Sciences*, 10(4), 553–572.
- de Andrade, F.M., Young, M.P., MacLeod, D., Hirons, L.C., Woolnough, S.J. & Black, E. (2021) Subseasonal precipitation prediction for Africa: forecast evaluation and sources of predictability. *Weather and Forecasting*, 36(1), 265–284.
- Dinku, T., Funk, C., Peterson, P., Maidment, R., Tadesse, T., Gadain, H. et al. (2018) Validation of the CHIRPS satellite rainfall estimates over eastern Africa. *Quarterly Journal of the Royal Meteorological Society*, 144(S1), 292–312. Portico. Available from: <https://doi.org/10.1002/qj.3244>
- Dutra, E., Magnusson, L., Wetterhall, F., Cloke, H.L., Balsamo, G., Bousssetta, S. et al. (2013) The 2010–2011 drought in the Horn of Africa in ECMWF reanalysis and seasonal forecast products. *International Journal of Climatology*, 33(7), 1720–1729.
- Endris, H.S., Hirons, L., Segele, Z.T., Gudoshava, M., Woolnough, S. & Artan, G.A. (2021) Evaluation of the skill of monthly precipitation forecasts from global prediction systems over the Greater Horn of Africa. *Weather and Forecasting*, 36, 1275–1298.
- Finney, D.L., Marsham, J.H., Walker, D.P., Birch, C.E., Woodhams, B.J., Jackson, L.S. et al. (2020) The effect of west-erlies on East African rainfall and the associated role of tropical cyclones and the Madden-Julian Oscillation. *Quarterly Journal of the Royal Meteorological Society*, 146(727), 647–664.
- Funk, C., Harrison, L., Shukla, S., Pomposi, C., Galu, G., Korecha, D. et al. (2018) Examining the role of unusually warm Indo-Pacific sea-surface temperatures in recent African droughts. *Quarterly Journal of the Royal Meteorological Society*, 144, 360–383.
- Funk, C., Hoell, A., Shukla, S., Blade, I., Liebmann, B., Roberts, J.B. et al. (2014) Predicting East African spring droughts using Pacific and Indian Ocean sea surface temperature indices. *Hydrology and Earth System Sciences*, 18(12), 4965–4978.
- Funk, C., Pedreros, D., Nicholson, S., Hoell, A., Korecha, D., Galu, G. et al. (2019) Examining the potential contributions of extreme “Western V” sea surface temperatures to the 2017 March–June East African Drought. In: *Bulletin of American Meteorological Society*. United States of America: AMS.
- Funk, C., Peterson, P., Landsfeld, M., Pedreros, D., Verdin, J., Shukla, S. et al. (2015) The climate hazards infrared precipitation with stations—a new environmental record for monitoring extremes. *Scientific Data*, 2(1), 1–21.
- Gottschalck, J., Wheeler, M., Weickmann, K., Vitart, F., Savage, N., Lin, H. et al. (2010) A framework for assessing operational Madden-Julian oscillation forecasts: a CLIVAR MJO working group project. *Bulletin of the American Meteorological Society*, 91(9), 1247–1258.
- Gudoshava, M. & Semazzi, F.H. (2019) Customization and validation of a regional climate model using satellite data over East Africa. *Atmosphere*, 10(6), 317.
- Gudoshava, M., Wanzala, M., Thompson, E., Mwesigwa, J., Endris, H.S., Segele, Z. et al. (2022) Application of real time S2S forecasts over Eastern Africa in the co-production of climate services. *Climate Services*, 27, 100319.
- Harrison, L., Way-Henthorne, J. & Funk, C. (2019) *Climate hazards center early estimates and the East Africa March-to-May 2019 drought*. Available at: <https://www.agrilinks.org/post/climate-hazards-center-early-estimates-and-east-africa-march-may-2019-drought> [Accessed 10th July 2021].
- Hersbach, H. (2019) ECMWF's ERA5 reanalysis extends back to 1979. *ECMWF Newsletter*, 158(1).
- Hersbach, H., Bell, B., Berrisford, P., Hirahara, S., Horányi, A., Muñoz-Sabater, J. et al. (2020) The ERA5 global reanalysis. *Quarterly Journal of the Royal Meteorological Society*, 146(730), 1999–2049.
- Hersbach, H., de Rosnay, P., Bell, B., Schepers, D., Simmons, A., Soci, C. et al. (2018) *Operational global reanalysis: progress, future directions and synergies with NWP*. Publisher ECMWF, ERA report series, p. 65.
- Hirons, L., Thompson, E., Dione, C., Indasi, V.S., Kilavi, M., Nkiaka, E. et al. (2021) Using co-production to improve the appropriate use of sub-seasonal forecasts in Africa. *Climate Services*, 23, 100246.
- Hirons, L., Wainwright, C.M., Nying'uro, P., Quaye, D., Ashong, J., Kiptum, C. et al. (2023) Experiences of co-producing sub-

- seasonal forecast products for agricultural application in Kenya and Ghana. *Weather*, 78(5), 148–153.
- Hogan, E., Shelly, A. & Xavier, P. (2015) The observed and modelled influence of the Madden–Julian Oscillation on East African rainfall. *Meteorological Applications*, 22(3), 459–469.
- Huffman, G.J., Bolvin, D.T., Nelkin, E.J., Wolff, D.B., Adler, R.F., Gu, G. et al. (2007) The TRMM Multisatellite Precipitation Analysis (TMPA): quasi-global, multiyear, combined-sensor precipitation estimates at fine scales. *Journal of Hydrometeorology*, 8(1), 38–55.
- Indeje, M., Semazzi, F.H. & Ogallo, L.J. (2000) ENSO signals in East African rainfall seasons. *International Journal of Climatology: A Journal of the Royal Meteorological Society*, 20(1), 19–46.
- Joyce, R.J., Janowiak, J.E., Arkin, P.A. & Xie, P. (2004) CMORPH: a method that produces global precipitation estimates from passive microwave and infrared data at high spatial and temporal resolution. *Journal of Hydrometeorology*, 5(3), 487–503.
- Kalnay, E., Kanamitsu, M., Kistler, R., Collins, W., Deaven, D., Gandin, L. et al. (1996) The NCEP/NCAR 40-year reanalysis project. *Bulletin of the American Meteorological Society*, 77, 437–472.
- Kilavi, M., MacLeod, D., Ambani, M., Robbins, J., Dankers, R., Graham, R. et al. (2018) Extreme rainfall and flooding over central Kenya including Nairobi city during the long-rains season 2018: causes, predictability, and potential for early warning and actions. *Atmosphere*, 9(12), 472.
- Kim, H., Janiga, M.A. & Pegion, K. (2019) MJO propagation processes and mean biases in the SubX and S2S reforecasts. *Journal of Geophysical Research: Atmospheres*, 124(16), 9314–9331.
- Kim, H.-M., Webster, P.J., Toma, V.E. & Kim, D. (2014) Predictability and prediction skill of the MJO in two operational forecasting systems. *Journal of Climate*, 27(14), 5364–5378. Available from: <https://doi.org/10.1175/jcli-d-13-00480.1>
- Knapp, K.R., Diamond, H.J., Kossin, J.P., Kruk, M.C. & Schreck, C.J. (2018) *International best track archive for climate stewardship (IBTrACS) project, version 4*. Washington: NOAA National Centers for Environmental Information. Available from: <https://doi.org/10.25921/82ty-9e16>
- Kolstad, E.W. (2021) Prediction and precursors of Idai and 38 other tropical cyclones and storms in the Mozambique channel. *Quarterly Journal of the Royal Meteorological Society*, 147(734), 45–57.
- Lee, C.Y., Camargo, S.J., Vitart, F., Sobel, A.H., Camp, J., Wang, S. et al. (2020) Subseasonal predictions of tropical cyclone occurrence and ACE in the S2S dataset. *Weather and Forecasting*, 35(3), 921–938.
- Li, Y., Wu, J., Luo, J.J. & Yang, Y.M. (2022) Evaluating the eastward propagation of the MJO in CMIP5 and CMIP6 models based on a variety of diagnostics. *Journal of Climate*, 35(6), 1719–1743.
- Liebmann, B. & Smith, C.A. (1996) Description of a complete (interpolated) outgoing longwave radiation dataset. *Bulletin of the American Meteorological Society*, 77, 1275–1277.
- Lim, Y., Son, S.-W. & Kim, D. (2018) MJO prediction skill of the subseasonal-to-seasonal prediction models. *Journal of Climate*, 31(10), 4075–4094. Available from: <https://doi.org/10.1175/jcli-d-17-0545.1>
- MacLeod, D. (2018) Seasonal predictability of onset and cessation of the East African rains. *Weather and Climate Extremes*, 21, 27–35.
- MacLeod, D. (2019) *Seasonal forecast skill over the Greater Horn of Africa: a verification atlas of system 4 and SEAS5. Part 1: precipitation*. Available at: <https://www.ecmwf.int/node/18906> [Accessed 10th June 2022].
- MacLeod, D.A., Dankers, R., Graham, R., Guigma, K., Jenkins, L., Todd, M.C. et al. (2021) Drivers and subseasonal predictability of heavy rainfall in equatorial East Africa and relationship with flood risk. *Journal of Hydrometeorology*, 22(4), 887–903.
- Maidment, R.I., Grimes, D., Allan, R.P., Tarnavsky, E., Stringer, M., Hewison, T. et al. (2014) The 30 year TAMSAT African rainfall climatology and time series (TARCAT) data set. *Journal of Geophysical Research: Atmospheres*, 119(18), 10–619.
- Maraun, D. (2016) Bias correcting climate change simulations – a critical review. *Current Climate Change Reports*, 2, 211–220. Available from: <https://doi.org/10.1007/s40641-016-0050-x>
- Marshall, J., Houghton-Carr, H., Wainwright, C., Finney, D., Evans, B. & Okello, M. (2020) East Africa faces triple crisis of covid-19, locusts and floods. *Climate Home News*.
- Matthews, A.J. (2008) Primary and successive events in the Madden–Julian oscillation. *Quarterly Journal of the Royal Meteorological Society*, 134(631), 439–453.
- Maybee, B., Ward, N., Hiron, L.C. & Marshall, J.H. (2023) Importance of Madden–Julian oscillation phase to the interannual variability of East African rainfall. *Atmospheric Science Letters*, 24(5), e1148.
- Mutai, C.C. & Ward, M.N. (2000) East African rainfall and the tropical circulation/convection on intraseasonal to interannual timescales. *Journal of Climate*, 13, 3915–3939. Available from: [https://doi.org/10.1175/1520-0442\(2000\)013<3915:EARATT>2.0.CO;2](https://doi.org/10.1175/1520-0442(2000)013<3915:EARATT>2.0.CO;2)
- Mwangi, E., Wetterhall, F., Dutra, E., Di Giuseppe, F. & Pappenberger, F. (2014) Forecasting droughts in East Africa. *Hydrology and Earth System Sciences*, 18(2), 611–620. Available from: <https://doi.org/10.5194/hess-18-611-2014>
- NASA. (2018) *Dramatic flooding in Eastern Africa*. Available at: <https://earthobservatory.nasa.gov/images/92130/dramatic-flooding-in-eastern-africa> [Accessed 5th June 2023].
- Novella, N.S. & Thiaw, W.M. (2013) African rainfall climatology version 2 for famine early warning systems. *Journal of Applied Meteorology and Climatology*, 52(3), 588–606.
- Ogallo, L., Janowiak, J.E. & Halpert, M.S. (1988) Teleconnection between seasonal rainfall over East Africa and global sea surface temperature anomalies. *Journal of the Meteorological Society of Japan*, 66, 807–822. Available from: https://doi.org/10.2151/jmsj1965.66.6_807
- Palmer, P.I., Wainwright, C.M., Dong, B., Maidment, R.I., Wheeler, K.G., Gedney, N. et al. (2023) Drivers and impacts of Eastern African rainfall variability. *Nature Reviews Earth & Environment*, 4(4), 254–270.
- Park, S., Kang, D., Yoo, C., Im, J. & Lee, M.I. (2020) Recent ENSO influence on East African drought during rainy seasons through the synergistic use of satellite and reanalysis data. *ISPRS Journal of Photogrammetry and Remote Sensing*, 162, 17–26.
- Parker, D.J., Blyth, A.M., Woolnough, S.J., Dougill, A.J., Bain, C.L., de Coning, E. et al. (2022) The African SWIFT project: growing science capability to bring about a revolution in weather prediction. *Bulletin of the American Meteorological Society*, 103(2), E349–E369.

- Pohl, B. & Camberlin, P. (2006) Influence of the Madden–Julian oscillation on East African rainfall: II. March–May season extremes and interannual variability. *Quarterly Journal of the Royal Meteorological Society*, 132(621), 2541–2558.
- Reliefweb. (2020) *Special report: East Africa 2020 flood impacts on agriculture (updated May 19th, 2020)*. Available at: <https://reliefweb.int/report/somalia/special-report-east-africa-2020-flood-impacts-agriculture-updated-may-19th-2020> [Accessed 10th July 2023].
- Reynolds, R.W. (1993) Impact of Mount Pinatubo aerosols on satellite-derived sea surface temperatures. *Journal of Climate*, 6(4), 768–774.
- Saji, N.H., Goswami, B.N., Vinayachandran, P.N. & Yamagata, T. (1999) A dipole mode in the tropical Indian Ocean. *Nature*, 401(6751), 360–363.
- Salih, A.A., Baraibar, M., Mwangi, K.K. & Artan, G. (2020) Climate change and locust outbreak in East Africa. *Nature Climate Change*, 10(7), 584–585.
- Seo, K.H., Wang, W., Gottschalck, J., Zhang, Q., Schemm, J.K.E., Higgins, W.R. et al. (2009) Evaluation of MJO forecast skill from several statistical and dynamical forecast models. *Journal of Climate*, 22(9), 2372–2388.
- Talib, J., Taylor, C.M., Harris, B.L. & Wainwright, C.M. (2023) Surface-driven amplification of Madden–Julian oscillation circulation anomalies across East Africa and its influence on the Turkana jet. *Quarterly Journal of the Royal Meteorological Society*, 149(754), 1890–1912.
- Tarnavsky, E., Grimes, D., Maidment, R., Black, E., Allan, R.P., Stringer, M. et al. (2014) Extension of the TAMSAT satellite-based rainfall monitoring over Africa and from 1983 to present. *Journal of Applied Meteorology and Climatology*, 53(12), 2805–2822.
- Thorne, V., Coakeley, P., Grimes, D. & Dugdale, G. (2001) Comparison of TAMSAT and CPC rainfall estimates with raingauges, for southern Africa. *International Journal of Remote Sensing*, 22(10), 1951–1974.
- Vellinga, M. & Milton, S.F. (2018) Drivers of interannual variability of the East African “long rains”. *Quarterly Journal of the Royal Meteorological Society*, 144(712), 861–876.
- Vigaud, N., Tippett, M.K. & Robertson, A.W. (2018) Probabilistic skill of subseasonal precipitation forecasts for the East Africa–West Asia sector during September–May. *Weather and Forecasting*, 33(6), 1513–1532.
- Vitart, F., Ardilouze, C., Bonet, A., Brookshaw, A., Chen, M., Codorean, C. et al. (2017) The Subseasonal to Seasonal (S2S) prediction project database. *Bulletin of the American Meteorological Society*, 98, 163–173. Available from: <https://doi.org/10.1175/BAMS-D-16-0017.1>
- Vitart, F. & Molteni, F. (2010) Simulation of the Madden–Julian oscillation and its teleconnections in the ECMWF forecast system. *Quarterly Journal of the Royal Meteorological Society*, 136(649), 842–855.
- Wanzala, M.A. & Linda, O. (2020) *Recurring Floods in Eastern Africa amidst Projections of frequent and extreme climatic events for the region*. Kenya Nairobi: ICPAC Medium.
- Webster, P.J., Moore, A.M., Loschnigg, J.P. & Leben, R.R. (1999) Coupled ocean–atmosphere dynamics in the Indian Ocean during 1997–98. *Nature*, 401(6751), 356–360.
- Wheeler, M.C. & Hendon, H.H. (2004) An all-season real-time multivariate MJO index: development of an index for monitoring and prediction. *Monthly Weather Review*, 132(8), 1917–1932.
- White, C.J., Carlsen, H., Robertson, A.W., Klein, R.J.T., Lazo, J.K., Kumar, A. et al. (2017) Potential applications of subseasonal-to-seasonal (S2S) predictions. *Meteorological Applications*, 24(3), 315–325. Portico. Available from: <https://doi.org/10.1002/met.1654>
- Wood, A., Leung, L., Sridhar, V. & Lettenmaier, D. (2004) Hydrologic implications of dynamical and statistical approaches to downscaling climate model outputs. *Climatic Change*, 62, 189–216. Available from: <https://doi.org/10.1023/B:CLIM.0000013685.99609.9e>
- Zaitchik, B.F. (2017) Madden-Julian Oscillation impacts on tropical African precipitation. *Atmospheric Research*, 184, 88–102.

SUPPORTING INFORMATION

Additional supporting information can be found online in the Supporting Information section at the end of this article.

How to cite this article: Gudoshava, M., Nyinguro, P., Talib, J., Wainwright, C., Mwanthi, A., Hirons, L., de Andrade, F., Mutemi, J., Gitau, W., Thompson, E., Gacheru, J., Marsham, J., Endris, H. S., Woolnough, S., Segele, Z., Atheru, Z., & Artan, G. (2024). Drivers of sub-seasonal extreme rainfall and their representation in ECMWF forecasts during the Eastern African March-to-May seasons of 2018–2020. *Meteorological Applications*, 31(5), e70000. <https://doi.org/10.1002/met.70000>